Vol. 17, No. 2 (2018) 603-612
Revista Mexicana de Ingeniería Química

# ELECTRODEPOSITION OF NICKEL IN AN ACIDIC MEDIUM FROM POWDER OF BATTERIES MADE OF NICKEL METAL HYDRIDE (NiMH)

# ELECTRODEPÓSITO DE NÍQUEL EN MEDIO ÁCIDO A PARTIR DE POLVOS DE BATERÍAS DE NiMH (HIDRURO METALICO DE NÍQUEL)

B.G. Cuevas-González[1]*, C. Monterrubio-Badillo[2] , R. Cuenca-Álvarez[3]
[1]*Tecnológico de Estudios Superiores de Ecatepec, Av. Tecnológico S/N C.P. 55210 Col. Valle de Anáhuac, Ecatepec de Morelos, Edo de México.*
[2]*Centro de Investigación e Innovación Tecnológica, Instituto Politécnico Nacional Cerrada de Cecati s/n, Col. Santa Catarina, Del. Azcapotzalco, México D.F.*
[3]*Centro Mexicano para la Producción más Limpia, Instituto Politécnico Nacional, Av. Acueducto S/N Barrio la Laguna, Col. Ticoman, Del. Gustavo A. Madero, 07430.*
Received July 28, 2017; Accepted February 8, 2018

**Abstract**
This piece of work is focused on the evaluation of an alternate route to recover nickel from NiMH residual batteries beginning from the mechanical stage of disassembly, fragmentation and conditioning of powders by means of the process of mechanofusion and the stage of extraction of nickel from acidic electro deposition. By means of the process of mechanofusion, the properties of the particles are modified with a view to increasing the efficiency of the electrolytic treatment via the size control, particle form and the dispersion of species on a particle bed. The obtaining of metallic nickel was made at 50 mA/ $m^2$ at a temperature of 21°C via electrolysis with a constant potential producing a deposit of 295 ppm Ni.
*Keywords*: NiMH, Nickel, mechanofusion.

**Resumen**
Este trabajo se orienta a la evaluación de una ruta alternativa para recuperar Ni a partir de baterías de NiMH de desecho partiendo de la etapa mecánica del desensamble, la fragmentación, acondicionamiento de polvos por el proceso de mecanofusión y la etapa de extracción de níquel por electrodeposición ácida. A través del proceso de mecanofusión, las propiedades de las partículas son modificadas con vista a aumentar la eficiencia del tratamiento electrolítico, vía el control del tamaño, forma de las partículas y la dispersión de especies en un lecho de partículas. Los polvos obtenidos pueden entonces ser utilizados en disoluciones acuosas, a presión ambiente y temperaturas por debajo de 50 °C para formar depósitos por la reducción de los iones de Ni presentes en la solución electrolítica. La obtención de Ni metálico se realizó a 50 mA/ $m^2$ a 21°C, por electrólisis a un potencial constante produciendo un depósito de 295 ppm de Ni.
*Palabras clave*: NiMH, níquel, mecanofusión.

## 1 Introduction

Rechargeable batteries type AB, also known as NiMH are fabricated with metallic components such as nickel, cobalt and rare earths ( Pietrelli *et al*., 2002; Lupi and Pilone, 2002). The consumption of this type of batteries has had a constant increase worldwide in the last years due to the ever increasing use of portable devices like telephones, mobiles, portable computers also known as laptops, digital cameras as well as music and video players (Kopera ,2004; Müller and Friedrich, 2006; Tang *et al*., 2006). Also, others that stand out are hybrid and electric vehicles currently available on the market, all of which use exclusively batteries type NiMH (Nathira *et al*., 2008; Li, 2004). On the other hand, electronic devices like cellular and other domestic applications incorporate nanomaterials (NMs) that improve the dissipation of heat and electric conduction, among other properties. When these articles ended the shelf life, the child collected and sent them to a final disposal site where they concentrated a large amount of nanocontaminants in the environment that are transported mainly by the water currents (Cervantes-Avilés *et al*., 2017).This market is at present on the increase and will cause a production of an even larger number of NiMH

* *Corresponding author. E-mail*: bcuevas_2973@yahoo.com.mx
*doi: 10.24275/10.24275/uam/izt/dcbi/revmexingquim/2018v17n2/Cuevas* ; *issn-e*: 2395-8472

batteries (Lam and Louey, 2006; Fetcenko *et al*., 2007). At the end of their working life and when they are disposed of, the metals are susceptible of being recovered, all this can turn them into alternate forms of raw materials in the production of alloys based on Ni (Gavilán *et al*., 2009; Wiaux *et al*.,2001). This can lead to the development of manufacturing routes with the purpose of recycling the huge quantity of batteries that are disposed of thus recovering the economic benefit of extraction and reutilization of nickel (Lupi and Pasquali, 2005; Romano *et al*., 2004; Correia and Martín, 2004; Jovic *et al*., 2006). Due to all this, this piece of work is oriented towards the evaluation of an alternate way to recover Ni from NiMH batteries found as waste. All this consisting of the mechanical stage of the disassembly of batteries, the fragmentation and conditioning of powders via the mechanofusion process and the stage of extraction of nickel from acidic electrodeposition.

Through the mechanofusion process, the properties of particles are modified with a view to increasing the efficiency of the electrolytic treatment via the size control, particle form and the dispersion of species on a particle bed (Zhu *et al*., 2008; Chen *et al*., 2001; Reg, 2001). The powders obtained can then be utilized in aqueous solutions under ambient pressure and temperatures below 50 °C in order to form deposits by the reduction of nickel ions present in the electrolytic solution (Mohamedi *et al*., 2002).

## 2 Experimental

### 2.1 Materials

In order to identify the different elements present in the NiMH batteries, only one brand and the same model were selected.

### 2.2 Mechanical separation

The disassembly of batteries was made in an autogenous mill brand Stoneware model 010E-027, with an engine of 0.25 HP; it makes a container (internal diameter - 21 cm, internal height - 20cm) spin at 1725 revolutions per minute rpm. Due to this rotation, a chaotic action or flow is generated between the batteries leading to the rupture and removal of the plastic cover. By means of the magnetic separation, the metallic components are extracted for their fragmentation in the blade grinder (Oster, motor 2HP at 37000 rpm).

The magnetic separation is done again to remove the remnants of non-metallic materials.

Table 1. Operational parameters for the mechanofusion process

| Parameter | Value |
|---|---|
| Powder Mass | 50 g |
| Processing Time | 120 min |
| Compression Gap | 1.1 mm |
| Scraper Gap | 0.7 mm |
| Rotating Speed | 1400 rpm |

### 2.3 Conditioning of particles

The functionalization of particles is done making use of a mechanofusion reactor (described in a different part[MF Cuenca]), which consists in a static assemble of hydraulic hammers and drag blades located concentrically inside a cylindrical chamber in rotation ( Brieones, 2006; Velázquez, 2009). The powder introduced is dragged by the rotating chamber and form a bed of particles on the walls forcing it to pass through the air gap separation existing between the wall and the hammer. The powder is then subject to the effects of fragmentation by friction and lamination (Jartych *et al*., 2000).

Table 1 shows the operational parameters of the mechanofusion reactor to process the metallic powder got from the fragmentation of the batteries.

### 2.4 Electrodeposition

The process of nickel electrodeposition is done in accordance with the following reactions:

$$Ni^{2+} + 2e^- \rightarrow Ni^o \quad (1)$$

$$2H_3O + +2e^- \rightarrow H_2 + 2H_2O \quad (2)$$

In this study we will evaluate the development of these reactions in correlation to different electrolytes, (HCl, $HNO_3$ and $H_2SO_4$) in concentrations (0.1, 0.5 and 0.7M) over different substrata AISI 360L, aluminium, vitreous coal Pd and Pt (Egberts *et al*., 2006; Cheung *et al*., 1995; Kim *et al*., 2005).

In this way, the phenomena that take place are monitored by means of the following techniques: linear sweep voltammetry, cyclic voltammetry and static potentiometry.

The electrodeposition takes place at a constant temperature of 21 °C in electrochemical cells made of

Pyrex glass or Teflon. It consists in graphite electrodes, reference electrodes (Ag/AgCl) and counter electrode (susbtratum) in a electrolytic solution of $H_2SO_4$. This solution has the functions of being the electrolyte of the cell and dissolving the powder that comes from the mechanofusion reactor.

The influence of the chemical nature of the substrate as stainless steel (AISI 316L), aluminium, vitreous coal, palladium and platinum require that the surface of these substrates be prepared by conventional techniques of metallography like polishing using a flap SiC and mirror finish polishing (Ra=0.01 $\mu$m) with alumina powder; everything is cleaned by means of ultrasound for 5 minutes in distilled water and washed off in deionised water.

The electrochemical measurements take place utilizing a potentiostat/galvanostat with electrochemical impedance brand Autolab model PGSTAT 302 and controlled by the programme GPES/FRA.

The microstructure of the deposits, the form and the particle size are observed through a metallographic microscope brand Nikon model Eclipse. The analysis of images was realised with the programme Matrox Inspector version 2.2.

## 3 Discussion of results

### *3.1 Battery fragmentation*

With a view to obtaining a comparison, the manual disassemble of an NiMH battery was done. The table 2 presents the recovery of metallic material in a battery after each fragmentation process (Assumpc *et al*., 2006; Wu *et al*., 1999).

Figure 1 shows the spectrum of X-ray diffraction of each of the metallic components of the battery. The electrodes constitute nickel (JCPDS: 004-0850) and the separator of a mixture mostly rich in nickel with a nickel-iron compound (Kamacita, JCPDS: 037-0474), whilst the cover is constituted by the phases $Al_{1.06}LaNi_{3.94}$ (JCPDS: 033-024), ZrNiMn (JCPDS: 037-1200) and $La(OH)_3$ (JCPDS: 006-0585). In this way, the nickel is present in the 3 components of batteries and is susceptible of being extracted.

Table 2. Percentage in weight of the components of the battery before and after the fragmentation.

| | Metallic [% Weight] | Non-metallic [% Weight] |
|---|---|---|
| Pila unitaria (manual disassemble) | 90.44 | 8.66 |
| Autogenous mill | 78.6 | 20.5 |
| Blade grinder | 80.5 | 15.3 |

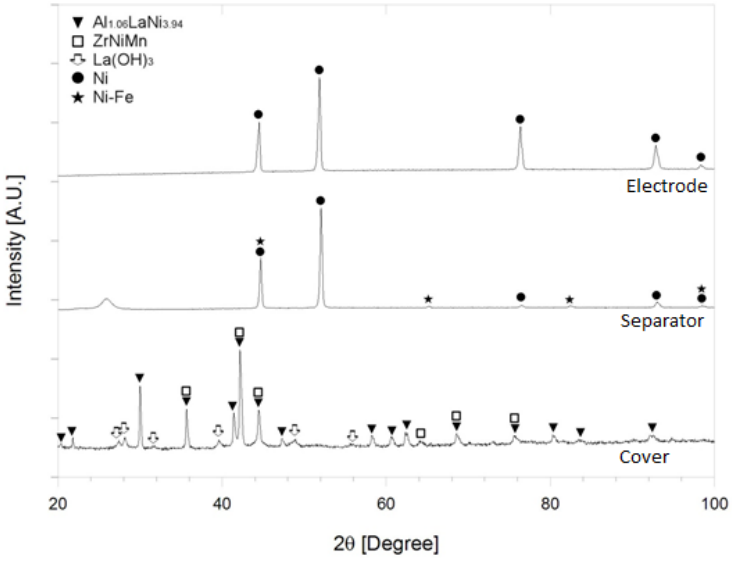


Fig. 1. DRX spectra of different components of batteries.

Table 3. Percentage in weight of the battery components before and after the fragmentation.

| Time MF processing [min] | $H_2SO_4$ Concentration [Mol] | | |
|---|---|---|---|
| | 0.1 | 0.5 | 0.7 |
| 0 | 54 | 71 | 74 |
| 30 | 22 | 31 | 29 |
| 45 | 14 | 12 | 11 |
| 60 | 8 | 5 | 3 |

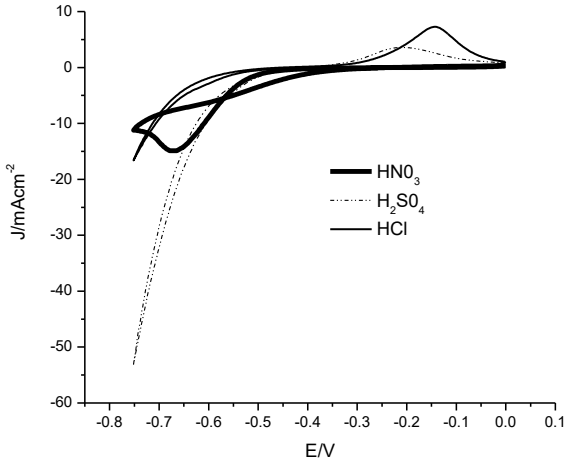


Fig. 2. Concentration 0.5 M; substratum: stainless steel AISI 316L.

## *3.2 Electrochemical extraction*

The powder obtained has to be dissolved into a solution of $H_2SO_4$ for the electrochemical extraction to take place (Pingwei *et al*., 1998). Nevertheless, the dissolution time works in function of the characteristics of the particles obtained by the fragmentation and the process of mechanofusion. Table 3 shows the variation in the dissolution time with respect to the time of the mechanofusion.The oxidation mechanism was a function of pH, by means of the generation of oxidants derived from the generation of hydroxyl radicals from water electrolysis (López-Ojeda *et al*., 2015).

## *3.3 Voltammetric study*

### *3.3.1 Influence of the electrolyte*

The dissolution of the NiMH powder in a particular way over the substratum AISI 360L in an acidic medium 0.5M of HCl, $HNO_3$ and $H_2SO_4$, is exposed in the voltammogram (figure 2) in which the oxide-reduction is presented.

Table 4. Flow density values and point of origin of the reduction for the different electrolytes.

| Electrolite | I ($mA/cm^2$) E = -0.75 V | P. of origin reduction $Ni^{2+} \rightarrow Ni$ E (V) |
|---|---|---|
| $HNO_3$, | -15.678 | -0.550 |
| $H_2SO_4$ | -53.678 | -0.453 |
| HCl | -16.653 | -0.516 |

In HCl and $H_2SO_4$ electrolytes peaks can be observed due to the effect of the oxidation in -0.35 to 0.5V and a reduction of -0.45 to -0.75 of nickel. The tendency for nickel reduction between -0.5 and -0.75 in the $HNO_3$ is well defined by showing the cathode electrolysis of the nickel reduction.

The values of the cyclic voltammetry of the different acidic electrolytes in a concentration of 0.5M substrata is reported in table 4 in which it can be determined that in the $H_2SO_4$ generates a larger flow while requiring less energy for the reduction of the nickel (Muñoz *et al*., 2003).

### *3.3.2 Influence of electrolyte concentration*

The coefficient of transference was evaluated in the different substrata; (a) AISI 360L, (b) Al, (c) vitreous coal, (d)Pt and (e) Pd in which the oxide-reduction behaviour in the electrode-electrolyte system is realised with a cyclical sweep with a start potential of 1.4 ending in -1.4 with a speed of 50 mV /sec. The electrolyte used was $H_2SO_4$ at 0.1, 0.5M, and 0.7M in which a density of flow intensity J is registered, the same that varies due to the substratum utilized against the potential applied.

In the voltammogram (Fig. 3a and d) of stainless steel and platinum, a peak from 1 to 1.5 V is observed, which can be attributed to the oxygen evolution in the baseline of oxidation while the peak of reduction is not present. In figure (b) in the substratum of aluminum the oxide reduction is not defined and in figure (c) the vitreous coal presents a capacitive current that does

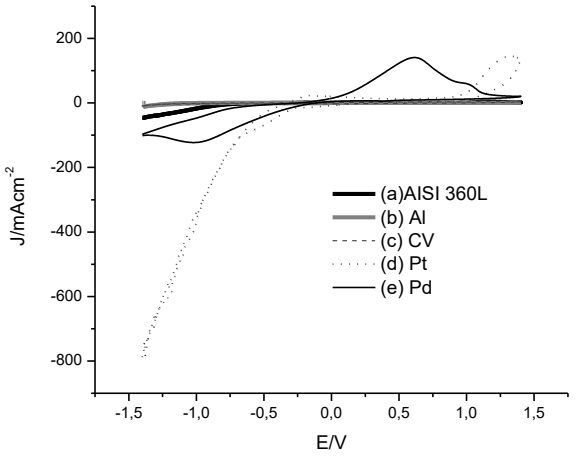


Fig. 3. Cyclic voltammogram in a potential of -1.4 a 1.4 V in different working electrodes (a) AISI 316 L, (b) Al, (c) vitreous coal, (d) Pt and (e) Pd in a solution 0.1M of $H_2SO_4$ at a sweep speed of $0.05 Vseg^{-1}$.

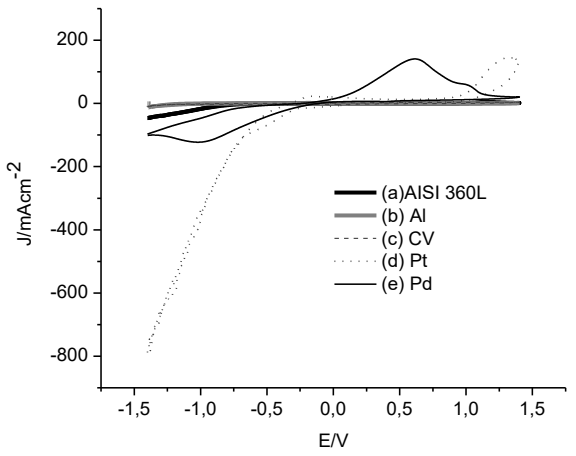


Fig. 4. Cyclic voltammograms obtained in the different types of working electrodes (a) AISI 316 L, (b)Al, (c)vitreous coal, (d) Pt and (e) Pd in a solution 0.5M of $H_2SO_4$ at a sweep speed of $0.05 Vseg^{-1}$.

not imply any chemical reaction (charge transfer), it only causes accumulation (or removal) because of the electric charges in the electrode and in the electrolytic solution that are close to the electrode, also known as 'non-faradic' current or 'double-layer' current. In figure 4 the nickel oxide-reduction in which a quasi-reversible reaction happens in the range between 0 and 1.5V; in this range, the oxidation of $Ni^{+2}$ and from 0 to -1.5 the reduction to Ni°. We can establish that the palladium when in an electrolytic concentration is the best substratum for the oxidation-reduction of nickel.

The electrolyte $H_2SO_4$ at a concentration of 0.5M was evaluated (figure 4) showing a maximum value which can be interpreted in the appearance of a maximum electronegative potential in figure 5a between 1.25 V and -0.5V for stainless glass and from -0.25 to -1 palladium fig.(e). Apart from an intersection of cathodic and anodic parts which is found from -0.5V to 1V and from -0.25 to 1.5V respectively; this one vanishes to zero where there is no electrolysis; among these slopes of curves, these curves represent the transition of the oxidised state to a reduced one in which the formation of a state of passivation of $Ni(OH)_2$ and NiO, characteristic of the deposits of Ni (Chang-Wei *et al*., 2009).

Table 5 summarizes the values of quantity of charge transferred in the substrata (Q), potential of

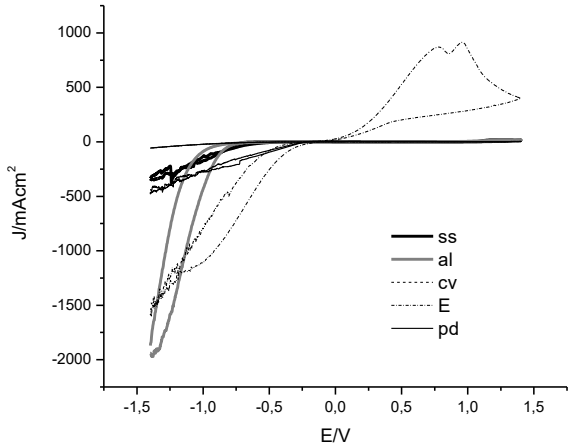


Fig. 5. Cyclic voltammograms obtained in different types of working electrodes (a) AISI 316 L, (b)Al, (c) vitreous coal (d) Pt and (e) Pd in a solution 0.7M of $H_2SO_4$ at a sweep speed of $0.05 Vseg^{-1}$.

cathodic peak (Epc) and the intensity of cathodic current (Ipc) in which the nickel reduction establishes stainless steel as the best substrate.

In the equation of the concentration 0.7M of $H_2SO_4$ in the voltammograms (Fig. 5a,b,c and e) it is recognizable a hydrogen evolution that does not enable the appreciation of nickel reduction; in figure 5d two peaks can be observed and attributed to the two states of nickel oxidation with an interval of E from 0 to 1.5 V.

Table 5. Performance of the substrates in the electrolyte medium at 0.5M of $H_2SO_4$.

| Substrate | Q Coulomb | Epc V | Ipc mA/cm$^{-2}$ |
|---|---|---|---|
| AISI 316L | 2.108e-02 | -1.00 | -22.97 |
| Al | - | - | - |
| CV | - | - | - |
| Pt | - | - | - |
| Pd | 3.769e-03 | -0.58 | -29.51 |

Table 6. Linear voltammetry $H_2SO_4$ 0.5M with a potential of -1.4 a 1.4 V.

| Substratum | Q Coulomb | Epc V | Ipc mA/cm$^{-2}$ |
|---|---|---|---|
| AISI 316L | 2.118e-02 | -1.00 | -27.18 |
| Al | - | - | - |
| CV | - | - | - |
| Pt | 3.58e-0.4 | -0.68 | -50.71 |
| Pd | 3.607-03 | -0.58 | -34.94 |

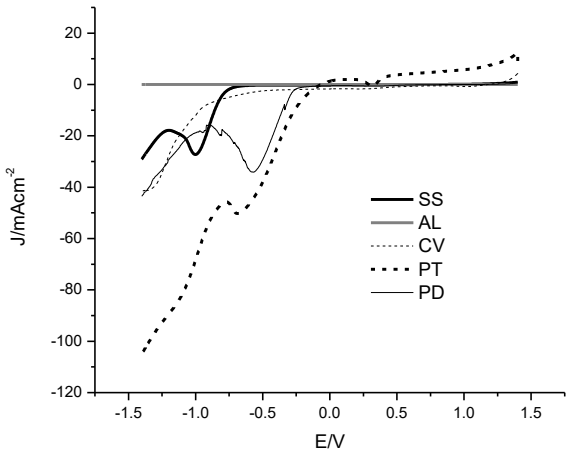


Fig. 6. Kinetic reaction (linear voltammetry) V=2mv/sec.

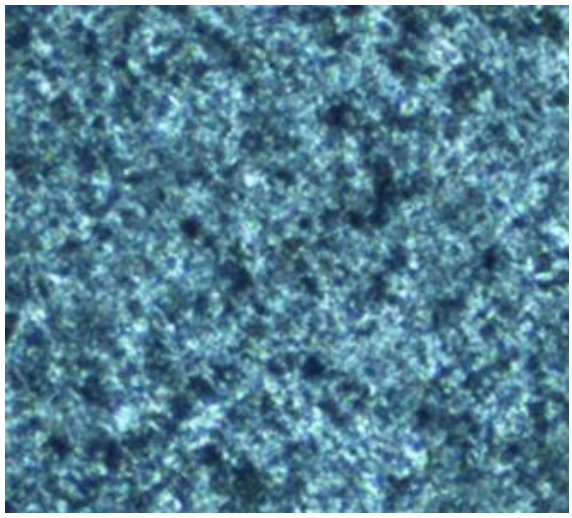

Fig. 7. Aspects of Ni deposits obtained by means of potentiometry.

### *3.3.3 Kinetic reaction by linear voltammetry*

In figure 6, it is represented the kinetic reaction in the electrolyte 0.5M $H_2SO_4$ followed by linear voltammetry of cathodic reduction for the working electrodes of AISI 316L aluminium, vitreous coal, palladium and platinum at a sweep rate from 1.40 to -1.4 with a flow relation of V=2mv/sec.

In table 6, data Q (charge) is extracted from the graph shown in figure 8; in this graph the minimum potential and least quantity of energy is followed by Pt while in third position in terms of quantity of energy required for the reduction of Ni.

## *3.4 Nickel deposit*

Although the analysis by voltammetry reveals that the Palladium is the most efficient material for the nickel deposit, it is preferable to employ the iron substrate AISI 360L for a number of reasons such as: accessibility of cost, the fact that it presents an acceptable behaviour in terms of mass transfer and, finally, the Ni deposits are easily removed with a view to an easy recovery of the metal (Velázquez-García, 2009).

At a flow density of 50 mA/cm$^2$ with a flow intensity of 0.17 A in a time lapse of 15 mins, the electrolysis takes place at 25°C in a solution without agitation in 0.5M $H_2SO_4$ of an adjusted electrolyte

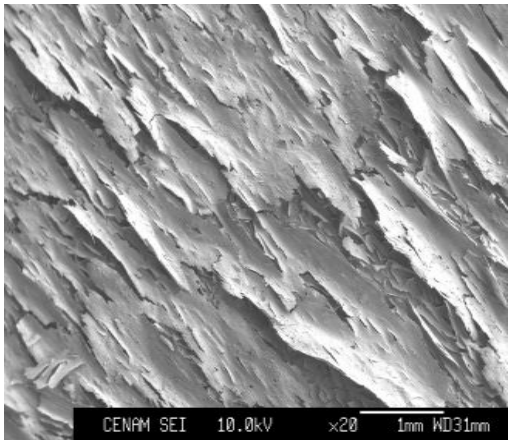


Fig. 8. Micrograph of Ni deposit.

in a pH=3 with $NH_4OH$, 295 ppm of Ni are obtained. Figure 7, presents a photo obtained with an optical microscope in which the electrodeposited material is observed with an homogeneous, compacted and globular-like deposit.

Figure 8 shows a micrograph obtained by a scanning electron microscope MEB brand JEOL JXA-8200WD/ED in order to appreciate the morphology which ratifies a scaled and irregular form with superimposed layers.

The more the number of magnifications (5000), the more defined the limits of grains can be perceived, figure 9A and at 25000 magnifications figure 9B a spongy morphology can be appreciated with a heterogeneous deposit with particles of up to 200nms.

Figure 10 presents the analysis of EDS (punctual microanalysis) of the nickel deposit obtained in the substrate AISI360L table 7 shows the semi-quantitative where it can be observed that the deposit consists of approximately a 100% of weight of nickel with a few impurities of Zn and S.

Figure 11 presents the spectrum of X-rays from the previous deposit with nickel detraction peaks only present in the interval $5\ ^\circ < 2\theta < 80\ ^\circ$ .

## Conclusions

The metallic parts of the batteries of NiMH were obtained by means of defragmentation in mechanical systems with a performance of efficiency of 85.5% in metallic parts.

The conditioning of particles by means of mechanofusion reduces the dissolution time up to a 50%.

Although the reduction-oxidation of Ni works in function of the substrate and the potential interval applied, the electrolyte of sulphuric acid generates a larger deposit flow and less energy for the nickel reduction to take place.

A) B)

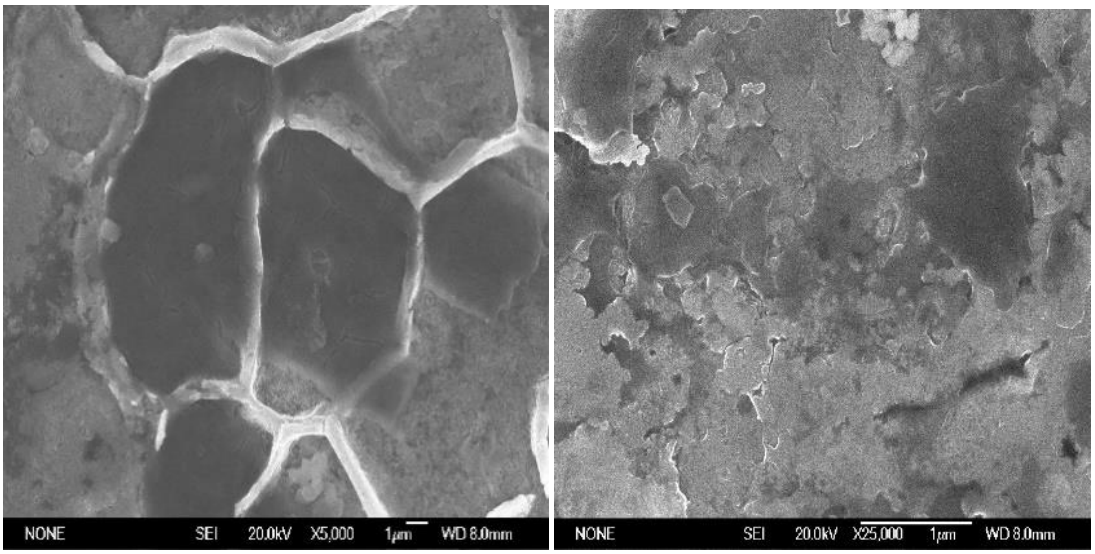


Fig. 9. Micrograph of the deposit of Ni at 5000 and 25000.

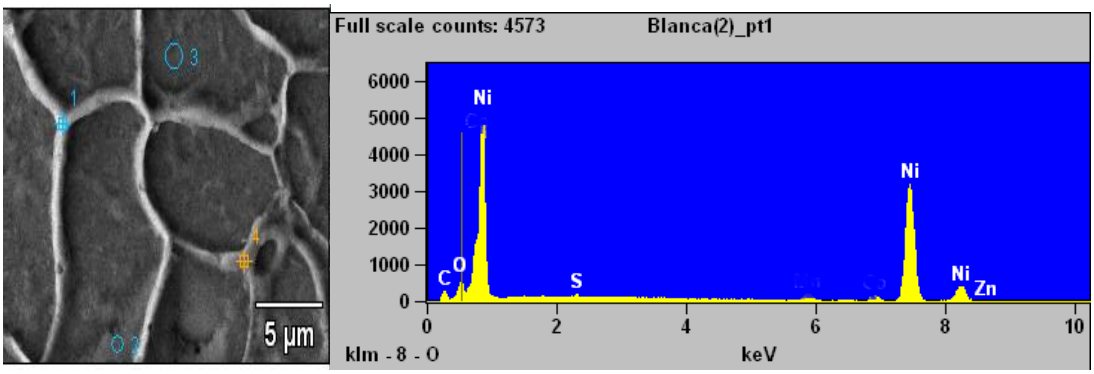


Fig. 10. Micrograph of the nickel deposit EDS.

Table 7. Analysis of the nickel deposit EDS

| Element | Line | Weight % | Weight % | Weight % | Atom % |
|---|---|---|---|---|---|
| S K | 1 | 0.47 | 0.58 | 0.93 | - |
| Ni K | 2 | 98.83 | 98.44 | 97.89 | 98.62 |
| Zn K | 3 | 0.70 | 0.88 | 1.18 | 1.38 |
| Total | 100.00 | 100.00 | 100.00 | 100.00 | |

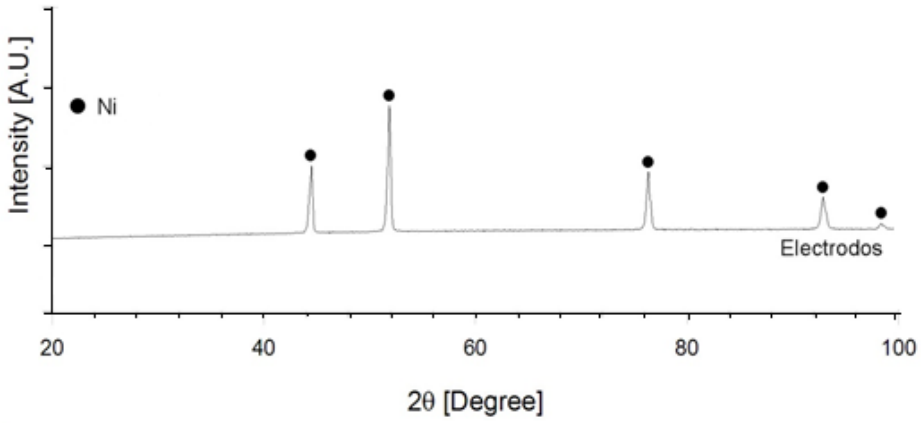


Fig. 11. DRX nickel deposit spectrum.

The Pd requires less energy to take place, followed by Pt and stainless steel in a solution of $H_2SO_4$ 0.5 M.

In a solution of $H_2SO_4$ 0.5 M better results can be perceived for the nickel reduction in comparison with 0.1 and 0.7M of $H_2SO_4$. With 0.1M no reduction peak can be observed and with 0.7M the reaction of hydrogen generation is favoured masking the reaction of nickel reduction.

Stainless steel is an alternative to be used as substratum in order to make the deposit at a large scale due to the fact that the cathodic activity is compared to that of Pd and Pl, which are better catalysts for the electrochemical reactions, yet more economical.

The obtaining of metallic Ni was made at 50 mA/ $m^2$ a 21°C by electrolysis at a constant potential producing an Ni deposit low in contaminants leaving 295 ppm.

## *Acknowledgements*

To the Center of Technological Research and Innovation of the Instituto Politécnico Nacional for all the support and guidance to the research that lead to these results. We would also like to thank the Consejo Nacional de Ciencia y Tecnología for the scholarship (22919)

## References


Assumpc D.¸ Bertuol, Moura Bernardes A., Soares Tenório J.A. (2006). Spent NiMH batteries: Characterization and metal recovery through mechanical processing. *Journal of Power Sources 160*, 1465-1470.

Briones C. (2006). Análisis del mecanismo de recubrimiento cerámico sobre partículas metálicas por Mecanofusión. Tesis de Maestría CICATA-CIITEC-IPN. México.

Cervantes-Avilés, E. Souza-Brito, A. Bernal-Martínez, J. Antonio Reyes-Aguilera, G. de la Rosa, G. Cuevas-Rodríguez. (2017). Impacto de los nanocontaminantes en biorreactores aerobios para tratamiento de aguas residuales. *Revista Mexicana de Ingeniería Química 16*, 247-260.

Chang-Wei Su, Feng-Jiao He, Hui Ju, Yu-bin Zhang, Er-li Wang (2009). Electrodeposition of Ni, Fe and Ni-Fe alloys on a 316 stainless steel surface in a fluorborate bath. *Electrochimica Acta 54*, 6257-6263.

Cheung C., Djuanda F., Erb U., Palumbo G. (1995). Electrodeposition of nanocrystalline Ni-Fe alloys. *Nanostructured Materials 5*, 513-523.

Correia Angelina, Martín María Luisa (2004). Potencial impacto ambiental de la disposición final de baterías usadas en teléfonos celulares en vertederos municipales. *Ingeniería UC* -11.-003, 41-51.

Egberts P., Brodersen P., Hibbard G.D. (2006). Mesoscale structure in electrodeposited nanocrystalline Ni-Fe alloys. *Materials Science and Engineering 441*, 336-341.

Fetcenko M.A., Ovshinsky S.R., Reichman B., Young K., Fierro C., Koch J., Zallen A., Mays W., Ouchi T. (2007). Recent advances in NiMH battery technology. *Journal of Power Sources 165*, 544-551.

López-Ojeda G.C., Gutierrez-Lara M.R., Duran-Moreno A. (2015). Effect of pH on the electrochemical oxidation of phenol using a dimensionally stable anode of $SnO_2$-$Sb_2O_5$-$RuO_2$. *Revista Mexicana de Ingeneiria Química 14*, 237-452.

Gavilán-García A., Rojas-Bracho L., Barrera-Cordero J. (2009). *Las Pilas en México: un Diagnóstico Ambiental*. INE. México.

Jartych E., Zurawicz J.K., D. Oleszak,M. Pekala (2000). X-ray diffraction, magnetization and Mössbauer studies of nanocrystalline Fe-Ni alloys prepared by low- and high-energy ball milling. *Journal of Magnetic Materials 208*, 221.

John J.C. Kopera. (2004). *Inside the Nickel Metal Hydride Battery*, COBASYS. EE.U.U.

Jovic V.D., Jovic B.M., Pavlovic M.G. (2006), Electrodeposition of Ni, Co and Ni-Co alloy powders. *Electrochimica Acta 51*, 5468-5477.

Kim S.-H., Sohn H.-J., Joo Y.C., Kim Y.W., Yim T.H., Lee H.Y. (2005). Effect of saccharin addition on the microstructure of electrodeposited Fe-36 wt.% Ni alloy. *Surface and Coatings Technology 199*, 43-48.

Lam L.T., Louey R. (2006). VRLA Ultrabattery for high-rate partial-state-of-charge operation. *Journal of Power Sources 158*, 1140-1148.

Li X. H., Yang Z. (2004). Effects of sputtering conditions on the structure and magnetic properties of Ni-Fe films. *Materials Science and Engineering 106*, 41-45

Lupi C., Pasquali (2005). Nickel and cobalt recycling from lithium-ion batteries by electrochemical processes. *Waste Management 25*, 215-220

Lupi Carla, Pilone D. (2002). Ni-MH spent batteries: a raw material to produce Ni-Co alloys. *Waste Management 22*, 871- 874.

Mohamedi M., Nishizawa M., Lee Seo-Jae, Takahashi D. (2002). Microvoltammetric study of electrochemical properties of a single spherical nickel hydroxide particle. *International Journal of Hydrogen Energy 27*, 295-300.

Müller Tobias, Friedrich Bernd. (2006). Development of a recycling process for nickel-metal hydride batteries. *Journal of Power Sources 158*, 1498-1509

Muñoz A.G., Salinas D. R., Bessone J.B. (2003). First stages of Ni deposition onto vitreous carbon from sulfate solutions. *Thin Solid Films 429*, 119-128.

Nathira Begum S., Muralidharan V.S., Ahmed Basha C. (2009). Electrochemical investigations and characterization of a metal hydride alloy (MnNi3.6 Al 0.4 Co0.7 Mn0.3) for nickel metal hydride batteries. *Journal of Alloys and Compounds 467*, 124-129

Pietrelli L., Bellomo B., Fontana D., Montereali M.R. (2002). Rare earths recovery from NiMH spent batteries. *Hydrometallurgy 66*, 135-139.

Zhang P., Yokoyama T., Itabashi O., Suzuki T.M., Katsutoshi (1998). Inoue Hydrometallurgical process for recovery of metal values from spent lithium-ion secondary batteries. *Hydrometallurgy 50*, 61-75.

Reg D. (2001). Particle science and technology-a view at the millennium. *Powder Technology 119*, 45-57.

Renheng T., Qiyun L., Fangming X., Neng P., Ying W. (2006). Study on nanocrystalline rare earth Mg-based system hydrogen storage alloys with AB3-type. *Journal of Rare Earths 24*, 343-346.

Romano Espinosa D.C., Moura Bernardes A., Soares Tenório J.A. (2004). An overview on the current processes for the recycling of batteries. *Journal of Power Sources 135*, 311-319.

Velázquez-García J.J. (2009). Fabricación de depósitos compósitos por rociado térmico de partículas recubiertas por mecanofusión. Tesis de Maestría en Tecnología Avanzada, CIITEC-IPN. México.

Wenliang Chena, Rajesh N. Davea, Robert Pfeffera, Otis Waltonb, O.(2004). Numerical simulation of mechanofusion system. *Powder Technology 146*, 121-136.

Wiaux, J.P. Pistoia, G., Wiaux, J.P., Wolsky, S.P. (2001). *Used Battery Collection and Recycling*, Elsevier Science,

Wu M.S., Huang C.M., Wang Y.Y. *, C.C. (1999). Effects of surface modification of nickel hydroxide powder on the electrode performance of nickel/metal hydride batteries. *Electrochimica Acta 44*, 4007-4016

Zhu H.P., Zhou Z.Y., Yang R.Y., Yu A.B. (2008). Discrete particle simulation of particulate systems: A review of major applications and findings. *Chemical Engineering Science 63*, 5728-5770.